



Uncertainty of climate change impact on crop characteristics: a case study of Moghan plain in Iran

Ahmad Sharafati¹ · Mahmoud Moradi Tayyebi¹ · Elnaz Pezeshki² · Shamsuddin Shahid³

Received: 8 July 2021 / Accepted: 20 April 2022 / Published online: 3 May 2022
© The Author(s), under exclusive licence to Springer-Verlag GmbH Austria, part of Springer Nature 2022

Abstract

Crop yield is one of the most critical factors in the food security chain. Climate plays a crucial role in crop water productivity in rainfed and irrigated crop productions. Climate changes would significantly impact crop characteristics, especially in Iran, where water is the major constraint of crop production. This study assessed the impact of climate change on crop water productivity with related uncertainty. The global climate model simulations of rainfall and temperature were statistically downscaled using LARS-WG6 for climate projection. The projected climate was used in the FAO AquaCrop model to simulate the variability of crop characteristics (crop cycle length, crop yield, and water productivity) for the assessment of climate change effect on major crops for three future horizons (2021–2040, 2041–2060, 2061–2080). Results revealed an increase in wheat yield by 14–54% and a decrease of growth duration by 1–12%, leading to an increase in water productivity by 9–96% in the future compared to the base period (1985–2016). In contrast, reduction in corn and soybean yield by 1–5% and 2–6% and growth period by 1–5% and 3–12%, and thus, an increase in water productivity by 1–9% and 2–24%, respectively, were projected. The growth duration of all the major crops was projected to decrease due to a rise in temperature and an increase in crop water productivity in the study area. The results indicate a more favorable condition for crop agriculture in the study area under the projected climate.

1 Introduction

Climate change would affect all the sectors related to the economy, but it might be worst for agriculture (Alamgir et al. 2020). The combined effects of rising temperature, CO₂ concentration, hydrological extremes (such as droughts and floods), and a decrease in water availability due to climate change would significantly affect crop agriculture in all regions of the world (Chiotti and Johnston 1995). The Middle East will experience the most severe negative implications of climate change than other regions in the world (Waha et al. 2017; Khaleefa and Kamel 2021). The increase in temperature and decrease in rainfall has also been noticed in some Middle East areas (Sulaiman et al. 2018; Naganna

et al. 2020). A significant expansion of drylands due to climate change has been demonstrated in several studies (Noor et al. 2019; Salman et al. 2020; Hamed et al. 2021, 2022). Rises in hydrological extremes, particularly droughts, are already evident (Sowers et al. 2011; Hosseini et al. 2020), which are projected to intensify in the future. Eventually, these changes would alter the crop irrigation need, growth period, yield, and livelihood for farmers and national food security (Homsy et al. 2020; Arikan et al. 2021). Adaptation measures based on projected climate conditions are essential for sustaining crop yield and reducing climate change risk in crop agriculture (Maghrebi et al. 2020).

The crop cycle length, crop yield, and water productivity are the main features of a crop. The crop cycle length denotes the growing period, consisting of the initial, development, and mid- and late-seasons (Allen et al. 1998). Water productivity denotes the crop yield per cubic meter of water consumption (Cai and Rosegrant 2003). Climate change may affect evaporation, plant respiration, crop growing period, and yield. The increase or decrease in crop productivity depends on geography, climate, growing season, crop type, and growing method (rainfed or irrigated) (Kang et al. 2009). A higher concentration of CO₂ enhances photosynthesis and

✉ Ahmad Sharafati
asharafati@gmail.com; asharafati@srbiau.ac.ir

¹ Department of Civil Engineering, Science and Research Branch, Islamic Azad University, Tehran, Iran

² Integrated Coastal Sciences and Water Resources Center, East Carolina University, Greenville, NC 27858, USA

³ School of Civil Engineering, Faculty of Engineering, Universiti Teknologi Malaysia, Johor, 81310 Bahru, Malaysia

helps in plant growth. The positive effect of CO₂ is beneficial to some crops, especially C3 species (Reilly et al. 2007). The temperature rise shortens the growth periods of wheat and corn regardless of CO₂ concentration. However, the total dry matter decreases in both the crops for the simultaneous effect of temperature rise and higher CO₂ levels, which led to an increase in seed yield for wheat but a decrease for corn (Yano et al. 2007; Calzadilla et al. 2013)—estimated a reduction of food and agronomy production by 1.6% without considering the positive effect of CO₂ concentration. However, Shiferaw et al. (2013) reported an increase in crop productivity by 3% for both rainfed and irrigated crops with higher CO₂ concentration.

Climate change impact on crop productivity is usually estimated using a projection of climate variables by general circulation models (GCMs) (Lobell et al. 2005). Coarse spatial resolution is crucial for GCM output, making it essential to downscale to a target area for impact assessment. Several studies have evaluated the effectiveness of different downscaling methods such as dynamical and statistical approaches. Statistical downscaling based on the physical relationship between the GCM simulated and the local climate is easy to use and computationally inexpensive but reliable in climate projections (Sachindra et al. 2018). Therefore, it has been vastly employed in climate change modeling at local and regional scales. Several models, such as the Long Ashton Research Station Weather Generator (LARS-WG), can downscale the climate variables. The LARS-WG model uses the Markov chain for downscaling daily climate data such as temperature (minimum and maximum), precipitation, radiation, or sunshine at the point of interest (station) under current and future climate change scenarios and has been found suitable for climate change impact assessment in different sectors (Sharafati et al. 2020).

The impact of climate change on crops is generally investigated based on the physiological aspect of plant growth and development and crop production over the regional scale (Leemans and Solomon 1993). For instance, Lobell et al. (2005) assessed the changes in wheat yield in Mexico due to climate change and showed that the yield increment after 1980 due to changes in temperature and precipitation. Ludwig and Asseng (2006) reported a significant increase in wheat yield despite a reduction in rainfall and a temperature rise.

Heinemann et al. (2017) studied the changes in rainfed bean yield in a region of Brazil owing to climate change using twelve CMIP5 GCM simulated climate variables (e.g., precipitation, solar radiation, minimum, and maximum temperature) and showed higher variability in crop yield for RCP 8.5 (314–439 kg/ha) compared to RCP2.6 (267–272 kg/ha).

Yang et al. (2017) evaluated the changes in irrigated corn yield over Portugal owing to climate change using

the AquaCrop model and 4 M-MPI-ESM-LR/SMHI-RCA climate model for RCP4.5 and RCP8.5 and reported 17% yield reduction during 2021–2080 due to negligible positive effects of higher CO₂ concentration. Dubey and Sharma (2018) assessed the changes in the yield of corn, wheat, and barley in Banas plain of India under two RCP scenarios using the AquaCrop model and revealed an increase in yield of all three crops during 2021–2050 under both scenarios.

Globally, wheat is considered the most important crop as it plays a major role in global food security (FAO 2018). It provides about 20% of total protein and energy in the diet to the worldwide population (Shiferaw et al. 2013). It is the highest-produced crop in the last 50 years (FAOSTAT 2018). Corn is an important grain in tropical and temperate regions and is placed after wheat in the production and harvested area (FAOSTAT 2018). Soybean is the most valuable agricultural crop globally and is considered the most important crop after wheat and corn (FAOSTAT 2018). Variability in characteristics of these three strategic crops due to climate change is assessed in this study.

The agriculture in the Moghan plain is significantly influenced by the changes in climate patterns due to the direct relationship between crop physiology and meteorological variables. Hence, assessing climate change impacts crop characteristics in this area is crucial for decision-makers.

Though climate change impact on crop production is a major concern in agriculture, uncertainty in the impact due to climate projections is a key challenge in taking necessary adaptation measures. Uncertainties in climate projections mainly arise from climate models and emission scenarios that differ for different climatic variables (Khan et al. 2006; Sharafati and Zahabiyou 2014). Hence, this study uses a novel and practical approach to link global climate models and agricultural productivity. To reach this goal, the AquaCrop model was employed to simulate the changes in crop productivity due to changes in temperature and CO₂. Climate change projections are subjected to large uncertainties due to climate models and emission scenarios. Therefore, the proposed approach considers the uncertainty of climate change in projecting crop characteristics. The outcome of this study is beneficial for policymakers to manage the resources and decide on the most efficient policies for climate change adaptation.

The study was conducted for Moghan plain in Iran. Daily temperature and rainfall simulated by CMIP5 GCMs for different RCP scenarios were downscaled for the study area using LARS-WG6, subsequently used in the AquaCrop model to simulate the possible changes in yield, growing period, and water productivity of the crops.

2 Study area and data

Moghan plain, located in the north of Ardabil province in Iran, includes Pars Abad, Bile Savar, and Germei. Geographically, the Moghan plain is bounded by longitude 47° 20' E to 48° 25' E and latitude 39° 21' N to 39° 45' N (Fig. 1). The mean annual temperature and precipitation of the area are 15.2 °C and 271.2 mm, respectively. The highest precipitation occurs in October (34.7 mm) and the lowest in August (7.3 mm). The daily climate variables, including temperature (maximum and minimum) and precipitation data recorded for 1985–2016 at Pars Abas station in Moghan plain, were collected from the Iranian Meteorological Organization. The wheat, corn, and soybean yields in the study area for the period 2003 – 2013 were collected from the Ministry of Agriculture-Jahad (Ardebil branch).

3 Methodology

AquaCrop was employed to simulate three crop characteristics, crop cycle, crop yield, and water productivity for the base period (1985–2016) and three future horizons, including (2021–2040), (2041–2060), and (2061–2080).

The calibrating and validating stages were conducted using historical climate data from 1985 to 2016. LARS-WG6

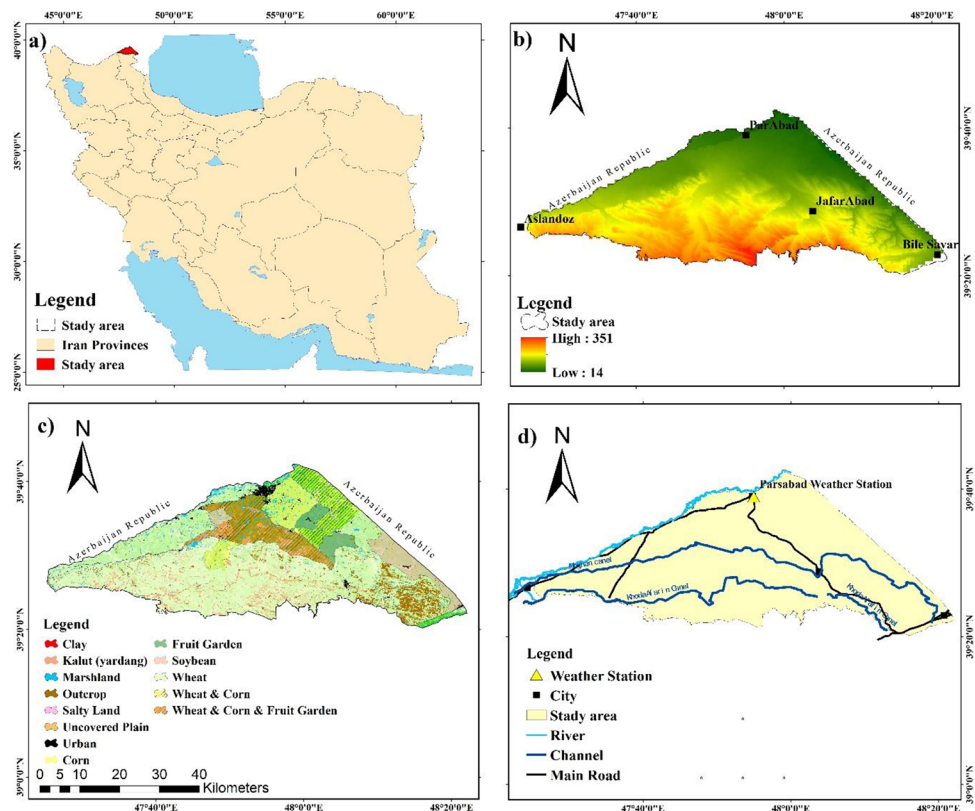
was used to generate the future climate based on four GCM simulations (HadGEM2-ES, EC-EARTH, MPI-ESM-MR, and MIROC5) for two scenarios, including RCP45 and RCP85. The projected climate data was used in the calibrated AquaCrop model for assessing the climate change impact on wheat, soybean, and corn characteristics.

Uncertainty in projections was estimated by comparing crop characteristics for the base period and future horizons. The procedure used to assess climate change on crop characteristics is shown using a flowchart in Fig. 2. Details of the methods and data used in the study are given in the following sections.

3.1 Climate downscaling using LARS-WG6

LARS-WG6 is a stochastic downscaling model which uses historical climate data for its calibration and validation and then the projection of the future climate of a location. The advantage of LARS-WG is that it can simulate daily climate data at the point of interest for the present and future climate conditions. It generates climate using the statistical characteristics of the observed climate of the location. For weather simulation at an ungauged location, weather generator parameters or the statistical characteristics of the climate variables are estimated for surrounding locations and then interpolated at the ungauged location. In this study, the inverse distance weighting method was used to interpolate

Fig. 1 The map of Moghan plain. **a** Location in Iran. **b** Digital elevation model. **c** The crop types. **d** Location of the Pars Abas station



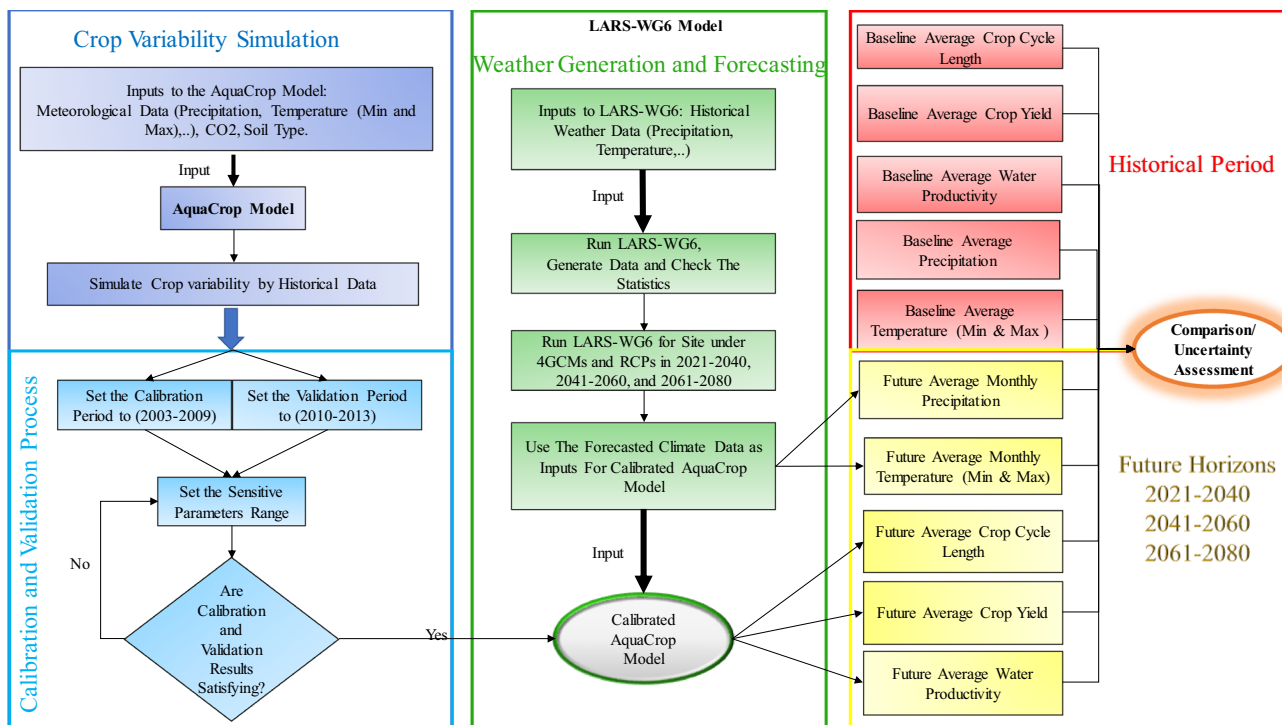


Fig. 2 Flowchart of the methodological framework used in the study

statistical parameters of climate variables. For the generation of future climate data, weather generator parameters are estimated from the GCM projected climate data for different RCP scenarios. Statistical characteristics of GCM simulated climate variables are interpolated to the site of interest to generate time series of climate variables.

In this study, LARS-WG6 was calibrated and validated with data from 1985 to 2016. The climate data for the base period was obtained from Iran Meteorological Organization. Simulations of four GCMs, MPI-ESM-MR, HadGEM2-ES, MIROC5, and EC-EARTH, for two scenarios, RCP45 and RCP85, were used in LARS-WG6 for the projection of future climates. The projections were made for three future periods, 2021 – 2040, 2041 – 2060, and 2061 – 2080. Table 1 provides a description of the employed GCMs used in this study.

3.2 AquaCrop

The AquaCrop was used to simulate the crop characteristics. The AquaCrop model has been widely utilized in previous studies to simulate the biomass and yield of maize (Qin et al. 2018), wheat (Dubey and Sharma 2018) and soybean (Silva et al. 2018). AquaCrop simulates daily crop growth from the various crop, soil, and climate parameters using a soil water balance method (FAO 2019). It is a robust and accurate tool for assessing crop characteristics for different climate and water stress scenarios (Steduto et al. 2009).

AquaCrop simulates total biomass (β) based on the water productivity (W) and the crop transpiration over the growing season (T) (Steduto et al. 2009):

$$\beta = W \sum T \tag{1}$$

Table 1 Description of GCMs and emission scenarios used in this study

Institution	Model	Emission scenario
A European community Earth-System Model	EC-EARTH	RCP4.5, RCP8.5
Met Office Hadley Centre, UK	HadGEM2-ES	RCP4.5, RCP8.5
Atmosphere and Ocean Research Institute (The University of Tokyo), National Institute for Environment Studies, and Japan Agency for Marine-Earth Science and Technology, Japan	MIROC5	RCP4.5, RCP8.5
Max Planck Institute for Meteorology, Germany	MPI-ESM-MR	RCP4.5, RCP8.5

The harvestable yield (γ) is estimated based on the β and Harvest Index (H) as follows:

$$\gamma = \beta \times H \tag{2}$$

Several statistical metrics have been widely used in different engineering applications (Amouamouha and Badalians Gholikandi 2017; Amouamouha and Gholikandi 2018; Gholikandi et al. 2021; Omeje et al. 2021) for assessing the models' performance. Herein, several indices, including RMSE, MAE, and CC, were used to measure the adequacy of the AquaCrop model over calibrating and validating stages as given in the following:

$$RMSE = \sqrt{\frac{1}{N_T} \sum_{j=1}^{N_T} (Y_{Obs} - Y_{Sim})^2} \tag{3}$$

$$MAE = \frac{1}{N_T} \sum_{j=1}^{N_T} |Y_{Obs} - Y_{Sim}| \tag{4}$$

$$CC = \frac{\sum_{j=1}^{N_T} (Y_{Obs} - \bar{Y}_{Obs})(Y_{Sim} - \bar{Y}_{Sim})}{\sqrt{\sum_{j=1}^{N_T} (Y_{Obs} - \bar{Y}_{Obs})^2 \sum_{j=1}^{N_T} (Y_{Sim} - \bar{Y}_{Sim})^2}} \tag{5}$$

where Y_{Obs} and Y_{Sim} denote the measured and simulated crop yield, respectively; \bar{Y}_{Obs} and \bar{Y}_{Sim} denote the measured and predicted mean of the crop yield, respectively; N_T is the total number of data.

The yield data of wheat, corn, and soybean were used for calibration (2003–2009) and validation (2010–2013) of AquaCrop model.

3.3 Quantification of uncertainty associated with climate change modeling

Systematic uncertainty is associated with large-scale models due to knowledge deficiency (Field and Barros 2014). This study quantified the uncertainty associated with GCMs and RCPs for projecting the climate variables and crop characteristics. A confidence band was estimated for GCMs' projected climate variables for different RCPs. An indicator named "R-factor" was used to quantify the uncertainty of projected climate variables (e.g., precipitation, temperature) and crop characteristics (e.g., crop cycle, crop yield, and water productivity) for different future horizons as follows (Sharafati and Pezeshki 2020):

$$R\ factor = \frac{\Delta}{\sigma} \tag{6}$$

where σ denotes the standard deviation of the baseline data and Δ can be computed as follows:

$$\Delta = \sum_{i=1}^m \frac{(UQ_i - LQ_i)}{m} \tag{7}$$

where m is the total number of observations, UQ_i and LQ_i are the upper quantile (90%) and lower quantile (10%) of the confidence band, respectively.

The methodology proposed in the present study is described in the following steps:

- i. Synoptic data (i.e., temperature, precipitation, and solar light) and crops data are collected.
- ii. The projected climate variables by selected GCMs for different RCPs are downscaled using the Lars-WG model.
- iii. Climate variables (min and max temperature, precipitation, CO₂) and observed crop characteristics are used to calibrate and validate the AquaCrop model.
- iv. Projected climate variables are imported to the calibrated AquaCrop model to project the crop characteristics for different future horizons.
- v. The uncertainty associated with projected crop characteristics is quantified using the R factor.

4 Results and discussion

4.1 Projection of weather variables

The accuracy of the LARS-WG6 model was validated for the base period. A comparison of observed and simulated rainfall and temperature by LARS-WG6 for the base period (1985–2016) is presented in Fig. 3.

Figure 3 shows that the LARS-WG6 has acceptable adequacy in simulating rainfall ($R^2 = 0.95$) and temperature ($R^2 = 0.99$) of the study area. Therefore, it was used to project future rainfall and temperature over Moghan plain. Four GCM simulations for RCP45 and RCP85 (a total of eight scenarios) were used to project future temperature and rainfall. Comparing the monthly average climate for three future periods with the base period is presented in Fig. 4. The GCMs projected both increases and decreases in rainfall for different months. The highest reduction in rainfall in September by –84% (3.87 mm compared to 24.5 mm during the base period) and the highest increase in October by 65% (53.57 mm compared to the base value of 32.5 mm). RCP85 projected both the highest decrease and increase in rainfall.

In the case of temperature, an increase was projected in temperature (maximum and minimum) over all the scenarios (Fig. 5). The projected increase in temperature was continuous with time. Generally, increases in temperature (maximum and minimum) were more in summer and relatively less in winter. The lowest rise in temperature was

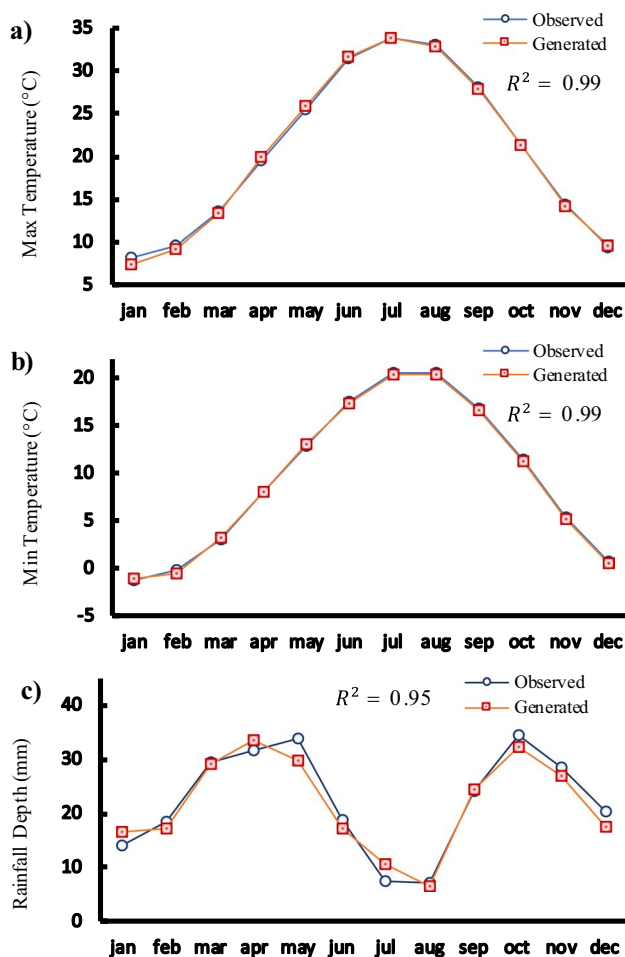


Fig. 3 Comparison of observed and simulated weather data obtained using LARS-WG6 for the base period, 1985–2016. **a** Maximum temperature (°C). **b** Minimum temperature (°C). **c** Rainfall depth (mm)

from December to February for all the models, emission scenarios, and future periods. The maximum temperature rise was highest (6.1 °C) in September (base period value was 28.1 °C) for RCP85 during 2061–2080, while it was lowest (0.7 °C) in January (base period value was 8.17 °C) for RCP85 during 2021–2040.

Table 2 briefly demonstrates the expected annual average temperature and rainfall changes projected by four GCMs for two RCPs during three future periods. The greatest changes in annual rainfall depth were observed in the far future (2061–2080) between –13.4 and 13.1%, while the lowest increase (5.4%) and decrease (–10%) were observed in the middle future (2041–2060) and near future (2021–2040), respectively.

The relative changes in annual maximum and minimum temperature revealed a marginal higher rise in maximum temperature than the minimum temperature during future

horizons. The changes in maximum temperature over the three future periods were in the range of 0.8 to 4.3 °C. EC-EARTH projected the lowest rise for RCP45 and the highest by HadGEM2_ES for RCP85. The projected minimum temperature increase was from 1.7 to 4.2 °C. The lowest increase in minimum temperature was projected by EC-EARTH for RCP45 while the highest by HadGEM2_ES for RCP85.

The uncertainty in projected rainfall and temperature was estimated using the confidence interval of the projections for the four models. The *R-factor* was estimated to quantify the uncertainty in projections of rainfall and temperature for different RCPs. Uncertainty in rainfall and temperature projections for both the RCPs were estimated separately for all the three future periods (Fig. 6). Results revealed a higher uncertainty in precipitation projections (*R-factor* = 0.35–0.68) than temperature projections (*R-factor* = 0.05–0.14). The larger uncertainty band for precipitation was due to both increase and decrease in average precipitation in different months (Fig. 6 a and b). Overall, an increase in precipitation in April, May, and June and a decrease in September for both RCPs and all horizons were projected with higher confidence. The highest uncertainty in projected precipitation for all the RCPs and future periods was for the fall months (September–November). Uncertainty in precipitation projection for RCP85 was more for early and far futures, while the uncertainty in precipitation projection for RCP45 was higher for the middle future. Furthermore, uncertainty in projections showed a gradual increase with time.

The uncertainty band of projected temperature for both RCPs showed a temperature rise (maximum and minimum) in all the months with high confidence. A significant difference in projected minimum and maximum temperature uncertainties were observed for RCPs and three future horizons. Like rainfall, the uncertainty in temperature projection for far-future (*R-factor* = 0.14) was higher than the other two periods for both RCPs.

The uncertainty associated with projected climate variables showed good agreement with other studies. Liu et al. (2021) found an increasing trend in the uncertainty of projected temperature with time over the City of Nur Sultan. Besides, Shin et al. (2021) indicated a higher variability in projected precipitation in the far future than in the near future. Barrow and Sauchyn (2019) reported higher uncertainty in projected temperature in the far future on the east coast of Canada. A study in the Himalayas also showed increasing uncertainty in the projected weather parameters with time for different RCPs. They also projected higher precipitation in the far future than in the near future (Sharma and Goyal 2020).

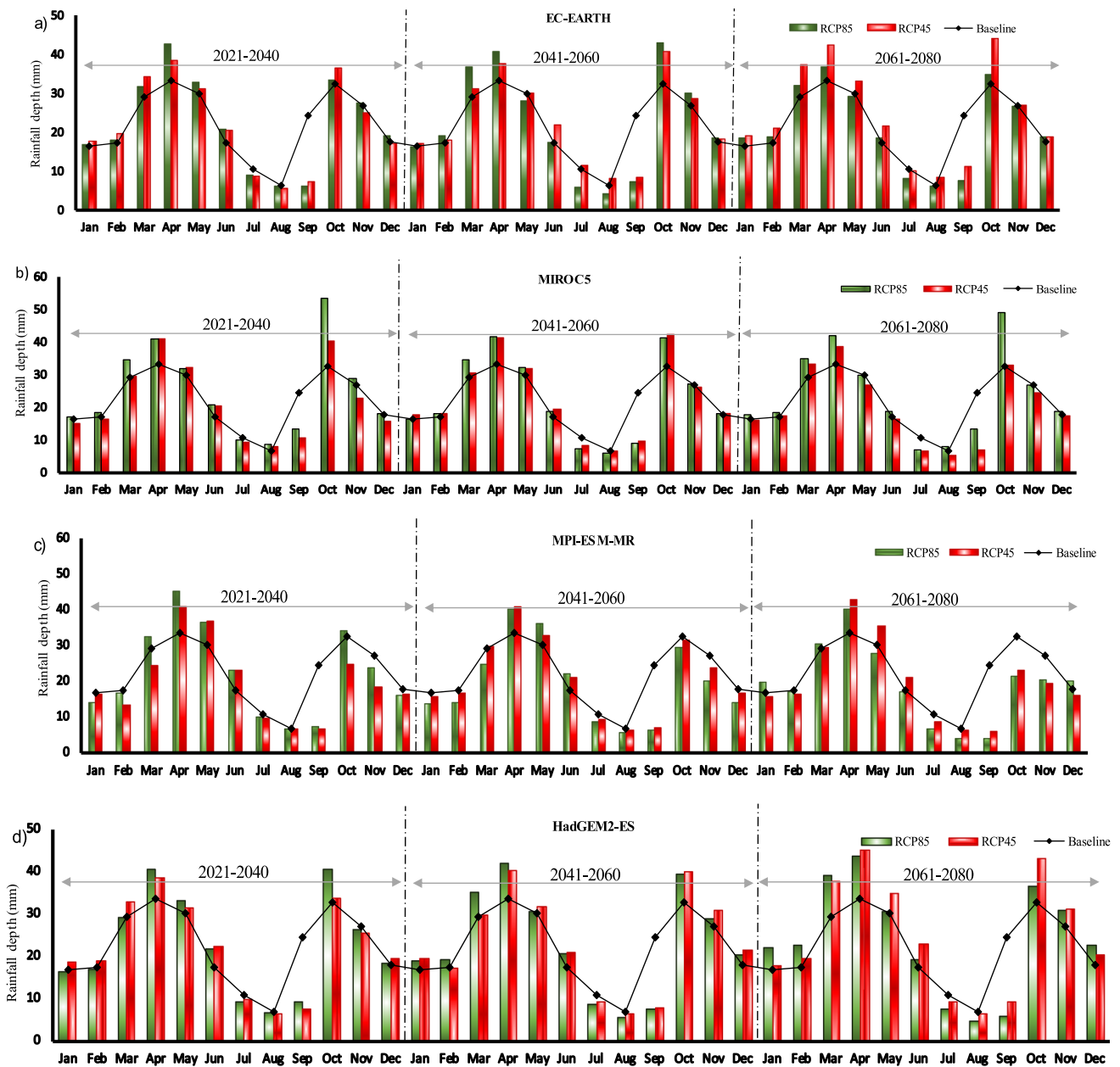


Fig. 4 Projected changes in rainfall in Moghan plain for eight scenarios and three future periods compared to the base period by a EC-EARTH, b MIROC5, c MPI-ESM-MR, and d HadGEM2-ES

4.2 AquaCrop model validity

Observed data of three crops for the period 2003–2009 was used for calibration, and the data for the period 2010–2013 was utilized to validate the AquaCrop model. The performance metrics (e.g., RMSE, MAE, and CC) obtained based on the observed and estimated crop yield are presented in Table 3.

Results show that AquaCrop has an adequate performance to simulate the crop features, where the CC was found high during both model calibration ($CC = 0.77 - 0.9$) and

validation ($CC = 0.68 - 0.8$). Besides, RMSE was reasonably low; 0.96–1.27 for wheat and corn, and 0.28–0.37 for soybean.

4.3 Climate change effect on crop characteristics

Calibrated AquaCrop model was used to simulate the yield, cycle length or growth period, and water productivity of wheat, corn, and soybean for future periods. Daily climate data for three future periods was employed for this purpose. The climate change impacts on crop variables for

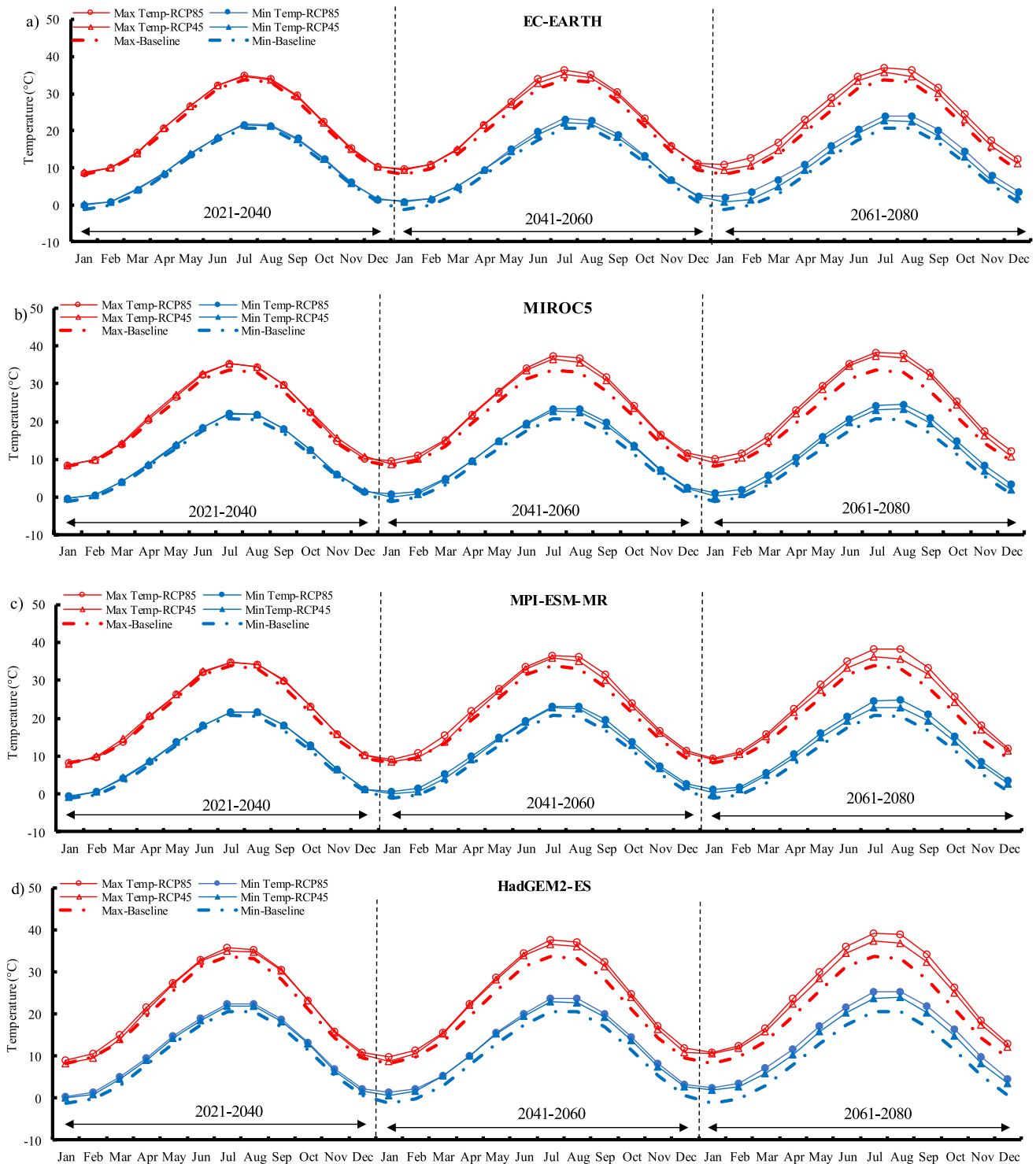


Fig. 5 Projected changes in maximum and minimum temperature in Moghan plain for eight scenarios and three future periods compared to the base period by **a** EC-EARTH, **b** MIROC5, **c** MPI-ESM-MR, and **d** HadGEM2-ES

20 cropping seasons were estimated. The changes in crop characteristics (crop yield, crop cycle length, and water productivity) in the future compared to the base period

Table 2 Projected changes in annual average of rainfall and daily temperature by the GCMs for two RCPs for three future periods

Variable	Future Horizon	MPI-ESM-MR		MIROC5		HadGEM2-ES		EC-EARTH		Maximum	Minimum
		RCP85	RCP45	RCP85	RCP45	RCP85	RCP45	RCP85	RCP45		
Annual rainfall depth changes (%)	2021–2040	1.0	-10.0	12.9	-0.1	2.2	0.9	0.4	-0.6	12.9	-10.0
	2041–2060	-10.7	-4.5	3.4	3.3	5.4	4.7	1.7	3.2	5.4	-10.7
	2061–2080	-13.4	-8.7	8.7	-7.4	8.6	13.1	-2.6	11.8	13.1	-13.4
Annual average maximum temperature changes (°C)	2021–2040	0.8	1.0	1.0	1.3	1.7	1.1	0.9	0.8	1.7	0.8
	2041–2060	2.2	1.4	2.6	2.0	2.9	2.2	1.9	1.5	2.9	1.4
	2061–2080	3.4	2.1	3.6	2.6	4.3	3.1	3.2	1.7	4.3	1.7
Annual average minimum temperature changes (°C)	2021–2040	0.9	0.9	0.9	1.0	1.7	1.2	1.0	0.9	1.7	0.9
	2041–2060	2.1	1.4	2.2	1.7	2.7	2.1	2.0	1.5	2.7	1.4
	2061–2080	3.1	2.0	3.1	2.0	4.2	3.0	3.3	1.7	4.2	1.7

The annual average rainfall depth, maximum temperature, and minimum temperature are 263(mm), 20.6 (°C), and 9.6 (°C), respectively

were estimated. Besides, the uncertainty in the changes was assessed for each crop.

Table 4 summarizes the average changes in the growth period (in percentage) of the crops in future periods compared to the base period. The growth period of all the crops was projected to decrease by all the models for all scenarios and future periods. The average lengths of growing periods of wheat, corn, and soybean during the base period were 213.72, 134.84, and 134.81 days respectively. Table 5 shows a decrease in the crop growth period in the future in the range of -1 to -14%. The lowest decrease for wheat, corn, and soybean growth period was projected by MPI-ESM-MR-RCP85 (-1%), EC-EARTH-RCP45 (-5%), and EC-EARTH-RCP85 (-3%), respectively, during the near future, while the highest decrease was projected by Had-CEM2-ES in the range of -12 to -14% for all the crops in the far future. Overall, the reduction in the crop growing period was projected more for RCP85 compared to RCP45.

Table 5 shows the crop yields changes due to climate change in the Moghan plain. The average yields during the base period were 4.51, 5.27, and 2.10 t/ha for wheat, corn, and soybean, respectively. The projected wheat yield showed a gradual increase, while the corn yield gradually decreased with time. The soybean yield showed a decrease in the near future but a continuous increase continuously from the middle to the far futures for both the RCPs. Overall, the projections indicated an increase in wheat yield and a decrease in corn and soybean yields for both scenarios. The projected increase in wheat yield was in the range of 14 to 54%, while the projected decrease in corn and soybean yield was 0 to -5% and -6 to -10%, respectively.

In the Moghan plain, the difference in projected trends in crops yield may be due to the difference in the optimum temperature range of different crops. Wheat needs an optimum temperature range of 17–23 °C (Porter and Gawith 1999), and therefore, temperature rise contributes to its yield. Although corn requires an average temperature of 27–33 °C for the best yield (Sánchez et al. 2014), a relative decrease in projected corn yield in Moghan plain may be owing to the high increase (up to 4.3 °C) in maximum temperature in the grain filling period, which harms corn yield. The optimum temperature for soybean growing is 15–20 °C (Heinemann et al. 2006). Thus, higher temperatures during its growing period (April–September) would cause a decrease in the projected soybean yield. However, the decreasing trend in soybeans yield is much lighter due to the increasing trend in projected CO₂ concentration. This finding is similar to that found in other studies on soybean yield (Heinemann et al. 2006).

The changes in water productivity of wheat, corn, and soybean for three future periods for two RCP scenarios than the base period were also estimated using the AquaCrop model.

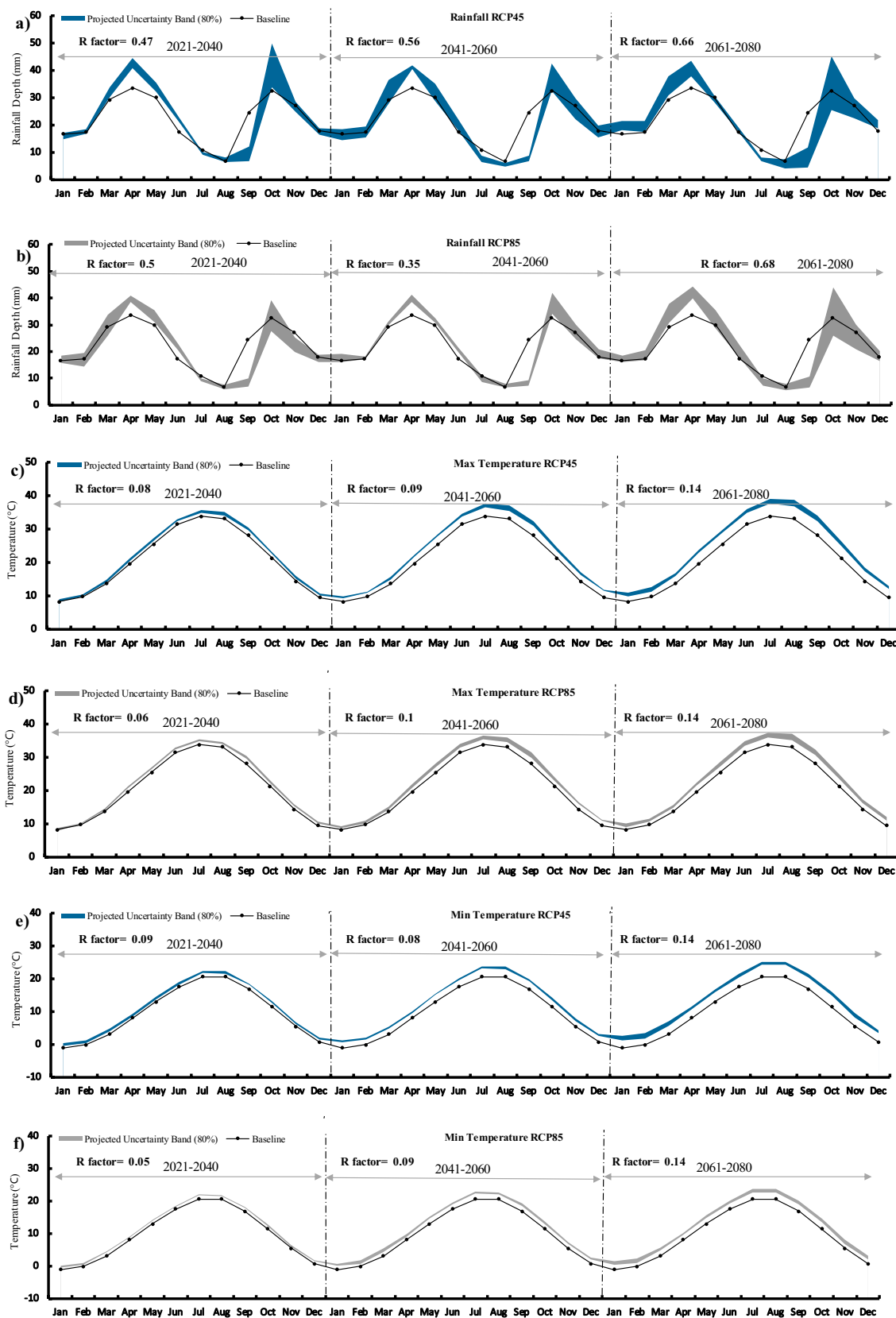


Fig. 6 Projected uncertainty in climate variables for RCP45 and RCP85 scenarios in Moghan plain for three future periods for **a, b** rainfall depth, **c, d** maximum temperature, and **e, f** minimum temperature

Water plays a vital role in crop yield, and therefore, water productivity is considered a crucial factor for ensuring food security with limited availability of water under climate change scenarios.

Table 6 summarizes the average changes in water productivity of three crops for three future periods under two RCPs. Average crop water productivity for wheat, corn, and soybean was 1.14, 1.09, and 0.4 kg/m³ for the base period. The projected crop water productivity increased for all the crops due to a decrease in the growth period. However, the increase was found highest for wheat (9–96%) and least for corn (–2–9%) and soybean (–1–24%).

4.4 Uncertainty associated with climate change impacts on crop characteristics

To quantify the uncertainty in projected yield, growth period, and water productivity of the crops, the interquartile range (IQR), which is the 3rd quartile (Q75%) minus 1st quartile(Q25%), was computed and presented using boxplots (Figs. 7, 8, 9). The uncertainty was estimated using the projections obtained using four GCMs for two RCPs. The height of the box (IQR value) represents the uncertainty in crops characteristics due to differences in GCM simulations.

Figure 7 a shows a lower uncertainty in the wheat growth period in the future (IQR = 3 ~ 8 days) than the base period (IQR = 9.5 days). The higher uncertainty in the base period compared to the future was due to less climate variability in the future than in the historical period. The uncertainty in projection was lower for RCP45 compared to RCP85. It was found to increase gradually with time for RCP45, but a decrease in the mid-period and then again increase in the far future (2061–2080) for RCP85. The uncertainty in the growth period of wheat was the lowest (3 days) during mid-future for RCP85, while it was highest (8 days) during far futures for RCP85.

Uncertainty of corn growth period is shown in Fig. 7b. Like wheat, the length of the corn cycle was found more variable (IQR = 6 days) for the base period than future periods (IQR = 2 ~ 3 days). The uncertainty of corn cycle length was found to increase gradually with time for RCP45, while it was found to decrease gradually for RCP85. The projected uncertainty of the corn growth period was the lowest for RCP85 during the far future (IQR = 2 days) and the highest for the same RCP in the near future (IQR = 3 days).

Similar results were also observed for soybean (Fig. 7c). Variation in the soybean growth period was more for the historical period (IQR = 5 days) than future periods (IQR = 2 ~ 4 days). The highest uncertainty in the soybean growth period was observed for RCP45 during the far future (IQR = 4 days) and the lowest for RCP85 during the far future (IQR = 2 days). A gradual increase in uncertainty with time for RCP45 was also observed, like wheat and corn.

Figure 8 compares the uncertainty of crop yield during base and future periods. Uncertainty in yield for the base period for all the crops was higher than the future due to higher yield variability in the base period. The increasing uncertainty was noticed for projected wheat and soybean yield for RCP85 while for all the crops for RCP45. The highest uncertainty of wheat, corn, and soybean's projected yield were observed 0.28, 0.12, and 0.06 ton/ha respectively for RCP45 in the far future, and the lowest, 0.19, 0.06, and 0.04 t/ha for the same RCP in the near future.

The boxplots presenting the uncertainty in the projected water productivity of the crops are shown in Fig. 9. Results show an increase in uncertainty in projected water productivity for wheat and no significant change for corn and soybean. The uncertainty in projected wheat water productivity was found to increase gradually with time for both RCPs. The highest uncertainty in projected wheat water productivity (IQR = 0.23kg/m³) was in the far future for RCP85. Uncertainty in projected corn water productivity was found to change very little in the future periods (IQR = 0.07 ~ 0.1kg/m³) compared to the base period (IQR = 0.11kg/m³). The highest uncertainty of corn water productivity was projected for RCP45 in mid future (IQR = 0.1kg/m³) and the lowest for RCP85 in the near future (IQR = 0.07kg/m³). Like wheat, the uncertainty in projected soybean water productivity was found to increase with time for both RCPs. The highest uncertainty in projected soybean water productivity was observed 0.05 kg/m³ for RCP85 in the far future and the smallest, 0.03 kg/m³ for RCP45 in the near future. The results indicate a negligible impact on the water productivity of corn and soybean.

5 Conclusion

The climate change impact on crop growth period, yield, and productivity were estimated for the Moghan plain of Iran. Precipitation and temperature projections of four GCMs for two RCP scenarios (RCP45 and RCP85) were downscaled using statistical downscaling software LARS-WG6. The AquaCrop model was used to simulate crop characteristics

Table 3 Crop yield statistics for the period 2003–2013 and corresponding estimation using AquaCrop model

Crop	Phase	Performance indices		
		CC	RMSE	MAE
Wheat	Calibration	0.84	0.96	0.81
	Validation	0.80	1.14	1.02
Corn	Calibration	0.77	1.27	1.20
	Validation	0.68	1.10	1.07
Soybean	Calibration	0.90	0.40	0.32
	Validation	0.74	0.37	0.28

Table 4 Changes in crop cycle length projected by different GCMs for three future periods under two scenarios

GCM	Scenario	Crop cycle length change (%)																		
		Crop cycle length (day)						Crop cycle length change (%)												
		Wheat		Corn		Soybean		Wheat		Corn		Soybean								
		2021–2040	2041–2060	2061–2080	2021–2040	2041–2060	2061–2080	2021–2040	2041–2060	2061–2080	2021–2040	2041–2060	2061–2080							
MPI-ESM-MR	RCP85	210.5	201.2	197	130.1	124.4	119.4	130.8	125.5	121.05	-1	-6	-8	-8	-4	-8	-11	-3	-7	-10
	RCP45	209.5	207.2	202	129.6	126.3	125.3	130.5	127.6	126.3	-2	-3	-5	-5	-4	-6	-7	-3	-5	-6
MIROC5	RCP85	209.2	200.4	194.5	128.7	122.9	119	129.6	124.4	120.7	-2	-6	-9	-9	-5	-9	-12	-4	-8	-10
	RCP45	207.8	204	202.8	128.4	125.3	122.8	129.4	126.3	124.3	-3	-5	-5	-5	-5	-7	-9	-4	-6	-8
HadGEM2-ES	RCP85	202.9	197.1	187.3	126.3	121.6	116.5	127.3	123	118.5	-5	-8	-12	-10	-6	-10	-14	-6	-9	-12
	RCP45	208.9	201	194.3	128.6	124.1	121.45	129.55	125.7	122.9	-2	-6	-9	-8	-5	-8	-10	-4	-7	-9
EC-EARTH	RCP85	208.6	200.6	189.8	129.9	123.6	120.3	130.75	125	122.2	-2	-6	-11	-11	-4	-8	-11	-3	-7	-9
	RCP45	207.2	202.2	201.8	129.8	127.7	125.9	130.6	128.8	127.2	-3	-5	-6	-6	-4	-5	-7	-3	-4	-6
Maximum		210.5	207.2	202.8	130.1	127.7	125.9	130.8	128.8	127.2	-1	-3	-5	-5	-4	-5	-7	-3	-4	-6
Minimum		202.9	197.1	187.2	126.3	121.6	116.5	127.3	123	118.5	-5	-8	-12	-10	-6	-10	-14	-6	-9	-12
Baseline		213.72			134.84			134.81												

Table 5 Changes in crop yield projected by different GCMs for three future periods under two scenarios

GCM	Scenario	Crop yield change (%)																		
		Crop yield (t/ha)						Crop yield change (%)												
		Wheat		Corn		Soybean		Wheat		Corn		Soybean								
		2021–2040	2041–2060	2061–2080	2021–2040	2041–2060	2061–2080	2021–2040	2041–2060	2061–2080	2021–2040	2041–2060	2061–2080							
MPI-ESM-MR	RCP85	5.3	5.9	6.7	5.3	5.2	5.1	2.0	2.1	2.3	17	32	48	0	-2	-4	-4	-3	1	9
	RCP45	5.1	5.6	5.9	5.2	5.2	5.2	2.0	2.1	2.1	14	24	30	0	-1	-1	-1	-5	0	1
MIROC5	RCP85	5.2	6.0	6.7	5.2	5.1	5.1	2.0	2.1	2.3	16	33	49	-1	-3	-4	-4	-4	0	8
	RCP45	5.2	5.6	5.7	5.2	5.2	5.1	2.0	2.1	2.1	14	24	27	-1	-2	-3	-3	-6	-2	0
HadGEM2-ES	RCP85	5.4	6.1	6.9	5.2	5.1	5.0	2.0	2.1	2.2	19	35	54	-2	-4	-5	-4	-6	-1	6
	RCP45	5.2	5.6	6.1	5.2	5.1	5.1	2.0	2.0	2.1	15	25	36	-1	-2	-4	-4	-6	-3	-2
EC-EARTH	RCP85	5.3	6.0	6.9	5.3	5.1	5.1	2.0	2.1	2.3	18	33	53	0	-2	-3	-3	-3	1	10
	RCP45	5.2	5.7	5.9	5.3	5.3	5.2	2.0	2.1	2.1	16	26	30	0	0	-1	-1	-5	0	2
Maximum		5.37	6.09	6.94	5.28	5.25	5.22	2.04	2.13	2.30	19	35	54	0	0	-1	-1	-3	1	10
Minimum		5.14	5.57	5.74	5.16	5.07	4.98	1.98	2.05	2.06	14	24	27	-2	-4	-5	-5	-6	-3	-2
Baseline		4.51			5.27			2.10												

Table 6 Changes in crop water productivity projected by different GCMs for three future periods under two scenarios

GCM	Scenario	Crop water productivity (kg/m ³)												Crop water productivity percent change (%)											
		Wheat			Corn			Soybean			Wheat			Corn			Soybean								
		2021–2040	2041–2060	2061–2080	2021–2040	2041–2060	2061–2080	2021–2040	2041–2060	2061–2080	2021–2040	2041–2060	2061–2080	2021–2040	2041–2060	2061–2080	2021–2040	2041–2060	2061–2080						
MPI-ESM-MR	RCP85	1.29	1.60	1.95	1.14	1.12	1.12	1.12	0.41	0.43	0.47	13	41	72	5	3	3	4	8	18					
	RCP45	1.25	1.42	1.59	1.12	1.13	1.12	0.40	0.43	0.43	10	25	40	3	4	4	1	7	8						
MIROC5	RCP85	1.26	1.58	1.94	1.12	1.09	1.11	0.41	0.42	0.46	11	39	71	3	0	2	3	5	16						
	RCP45	1.24	1.41	1.46	1.10	1.10	1.07	0.39	0.41	0.41	9	24	28	1	1	-2	-1	3	3						
HadGEM2-ES	RCP85	1.38	1.69	2.23	1.11	1.09	1.11	0.40	0.41	0.44	22	49	96	2	0	2	0	2	12						
	RCP45	1.29	1.49	1.77	1.12	1.10	1.10	0.40	0.41	0.41	14	31	56	3	1	1	0	2	4						
EC-EARTH	RCP85	1.30	1.59	2.12	1.14	1.15	1.19	0.42	0.44	0.49	14	40	87	5	6	9	5	12	24						
	RCP45	1.28	1.48	1.55	1.14	1.15	1.15	0.41	0.44	0.44	12	31	36	5	6	6	3	10	11						
Maximum		1.38	1.69	2.23	1.14	1.15	1.19	0.42	0.44	0.49	22	49	96	5	6	9	5	12	24						
Minimum		1.24	1.41	1.46	1.10	1.09	1.07	0.39	0.41	0.41	9	24	28	1	0	-2	-1	2	3						
Baseline		1.14			1.09			0.40																	

and estimate the changes in crop characteristics under the projected climate. The results revealed both increase and decrease in precipitation in different months, with the highest decrease in September (-84%) and the highest increase in October (65%) compared to base years. The projected temperature showed an increase in all the months for both scenarios, with the highest increase in summer and the lowest in winter.

The AquaCrop model projected a decrease in the growth period of wheat, corn, and soybean to an average of 202, 125, and 126 days. However, the projected yield was found to vary for different crops. The projection showed an increase in wheat and soybean yield by 29% and 1.5% and decreased corn yield by 2%. The projected crop water productivity for wheat, soybean, and corn indicated an increase by 36%, 3%, and 7%, respectively. The results indicate significant changes in the characteristics of three crops due to climate change. The impact will be higher for wheat, but it would be positive. Among the three characteristics of the crop, water productivity would be least affected by climate change, while the growth period would be most affected. The results obtained in this study can help in the management of water resources and crops and ensure food security in changing environment.

Acknowledgements The authors would like to reveal their gratitude and appreciation to the data providers, Iranian Meteorological Organization and Ministry of Agriculture-Jahad.

Author contribution Ahmad Sharafati proposed the topic, participated in coordination, aided in the interpretation of results, and paper editing. Mahmoud Moradi Tayyebi the review analysis, modeling and participated in drafting the manuscript. Elnaz Pezeshki carried out the investigation, and participated in drafting the manuscript. Shamsuddin Shahid carried out the validation, aided in the interpretation of results, and paper editing. All authors read and approved the final manuscript.

Data availability Please contact the corresponding author for data requests.

Code availability Please contact the corresponding author for code requests.

Declarations

Ethics approval Not applicable.

Consent to participate Not applicable.

Consent for publication Not applicable.

Conflict of interest The authors declare no competing interests.

Fig. 7 The uncertainty in the growth period during the base and three future periods for two RCP scenarios for **a** wheat, **b** corn, and **c** soybean

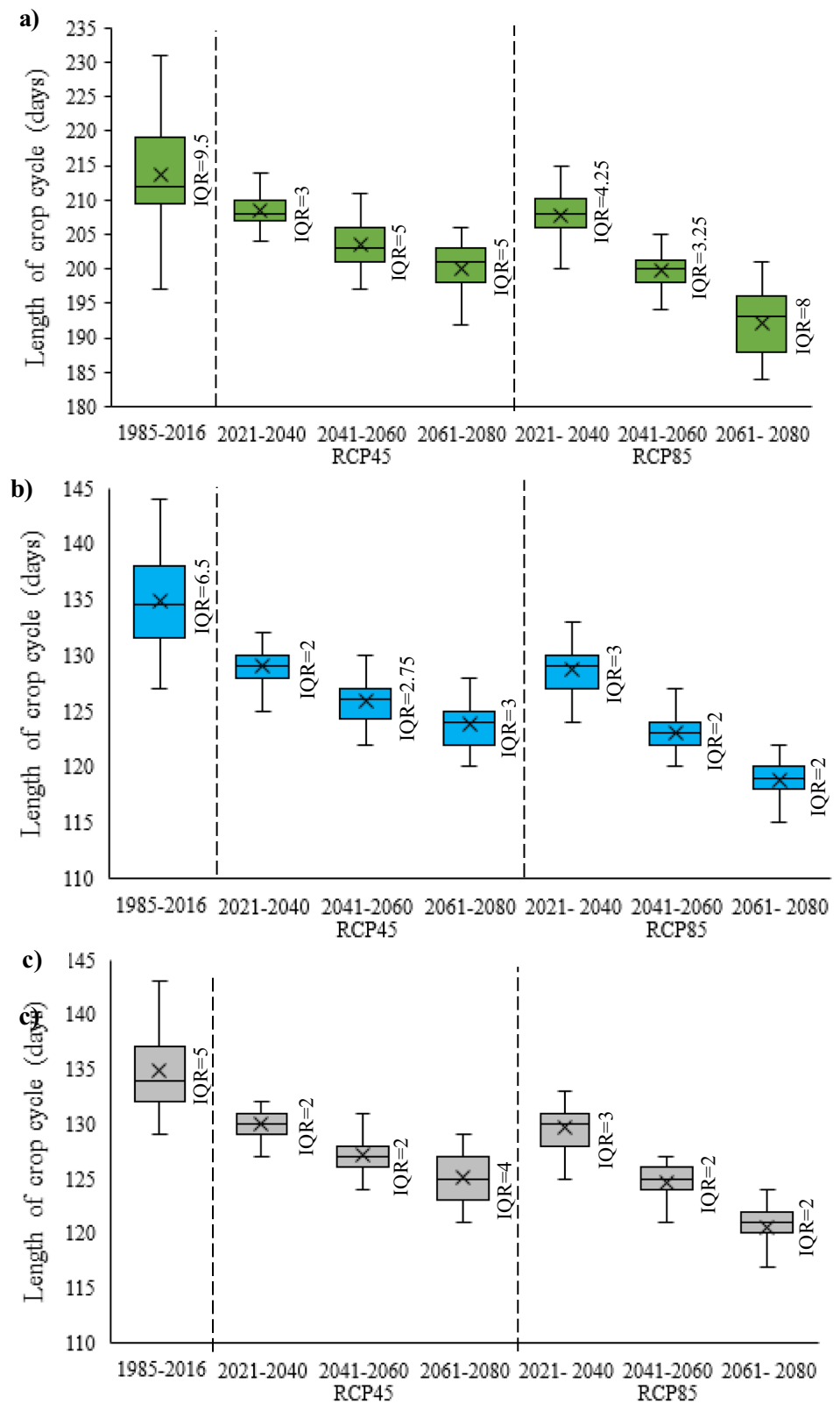


Fig. 8 The uncertainty in crop yield for the base and three future periods for two RCP scenarios for **a** wheat, **b** corn, and **c** soybean

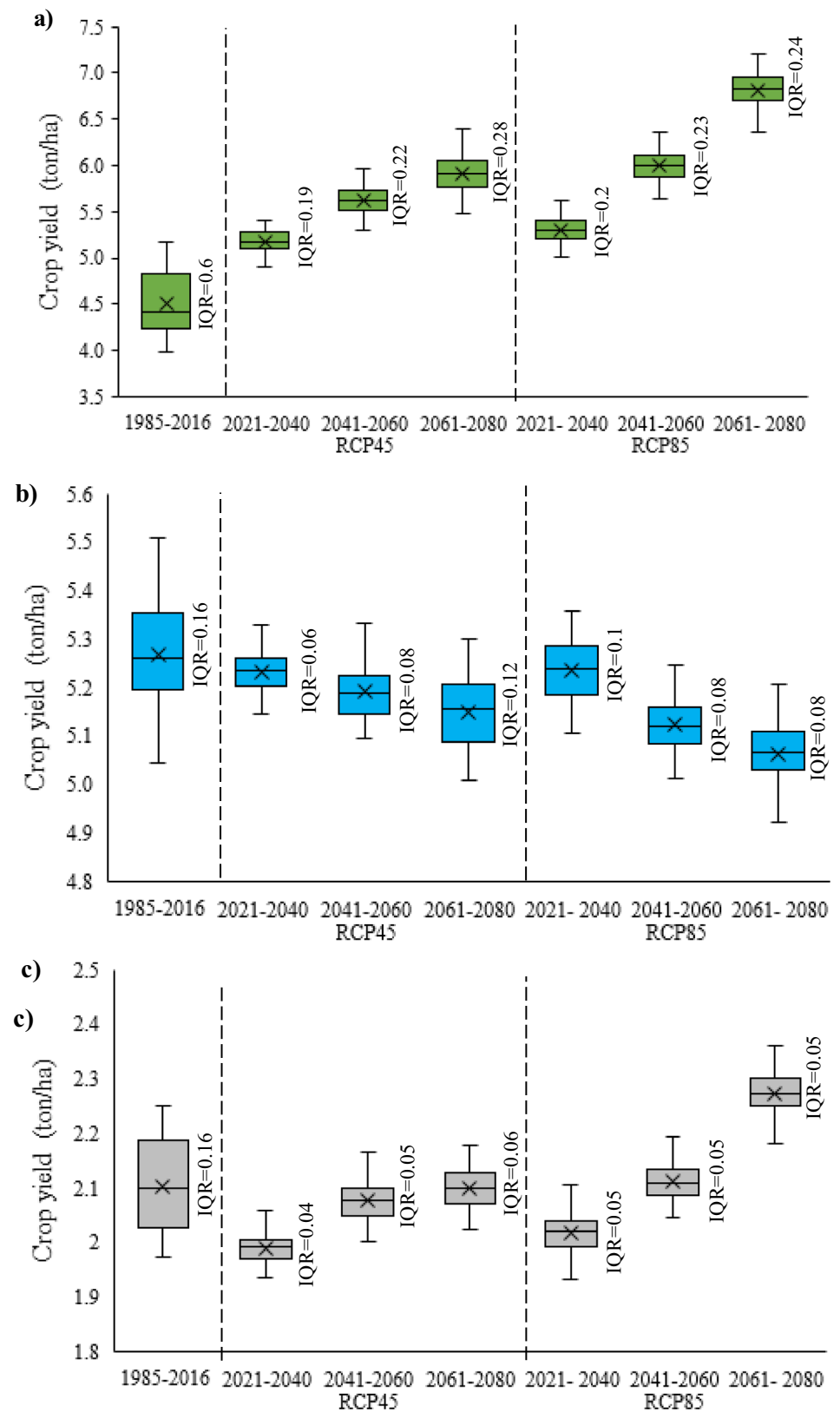
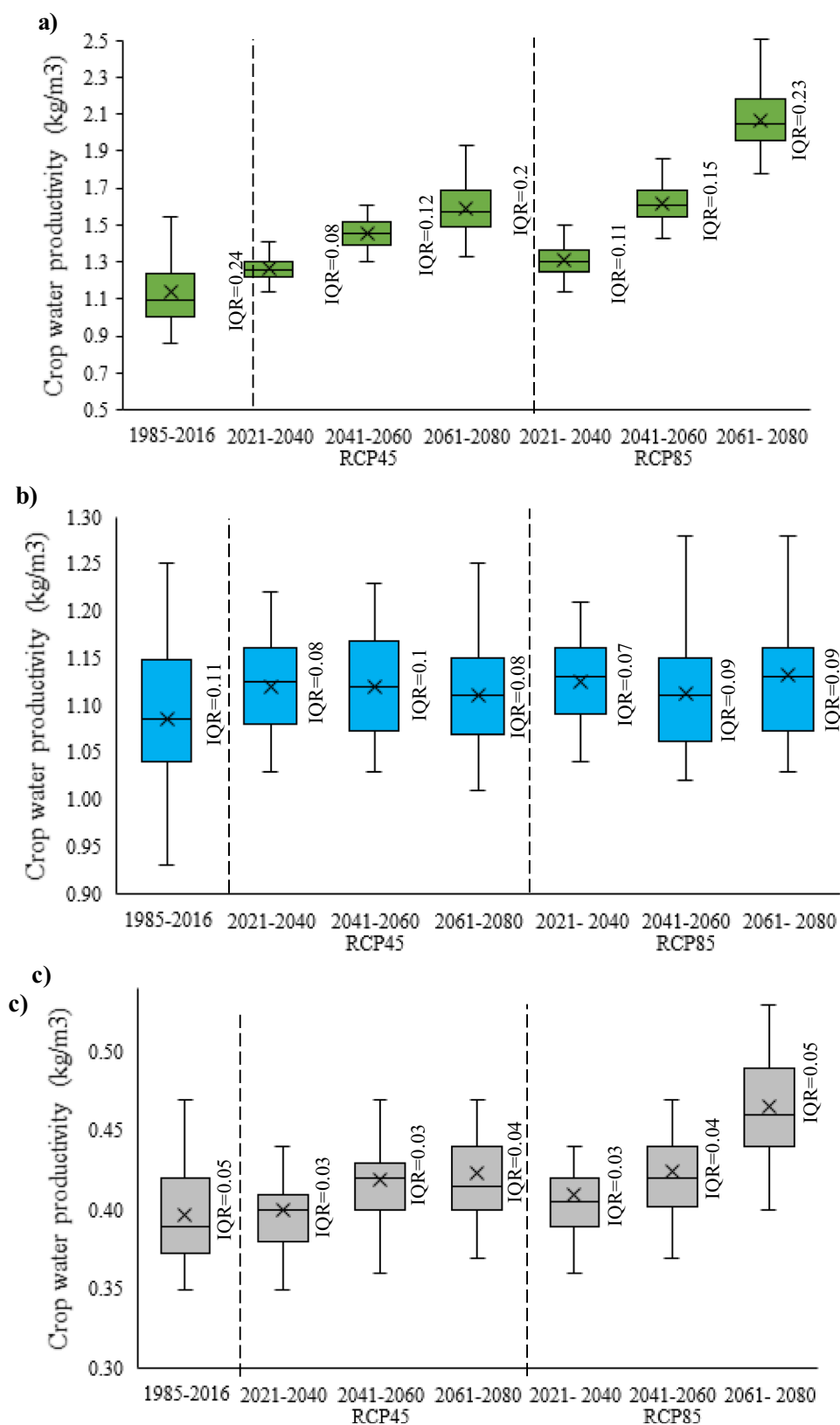


Fig. 9 The uncertainty in water productivity for the base and three future periods for two RCP scenarios for **a** wheat, **b** corn, and **c** soybean



References

Alamgir M, Khan N, Shahid S, et al (2020) Evaluating

- severity–area–frequency (SAF) of seasonal droughts in Bangladesh under climate change scenarios. *Stoch Environ Res Risk Assess* 1–18
- Allen RG, Pereira LS, Raes D, Smith M (1998) Crop evapotranspiration–Guidelines for computing crop water requirements–FAO Irrigation and drainage paper 56. Fao, Rome 300:D05109
- Amouamouha M, Badalians Gholikandi G (2017) Characterization and antibiofouling performance investigation of hydrophobic silver nanocomposite membranes: A comparative study. *Membranes (basel)* 7:64
- Amouamouha M, Gholikandi GB (2018) Assessment of anaerobic nanocomposite membrane bioreactor efficiency intensified by biogas backwash. *Chem Eng Process Intensif* 131:51–58
- Arikan BB, Jiechen L, Sabbah IID et al (2021) Dew Point Time Series Forecasting at the North Dakota. *Knowledge-Based Eng Sci* 2:24–34
- Barrow EM, Sauchyn DJ (2019) Uncertainty in climate projections and time of emergence of climate signals in the western Canadian Prairies. *Int J Climatol* 39(11):4358–4371
- Cai X, Rosegrant MW (2003) World water productivity: current situation and future options. In (Kijne JW, Barker R and Molden D, eds.) *Water productivity in agriculture: Limits and opportunities for improvement*
- Calzadilla A, Zhu T, Rehdanz K et al (2013) Economywide impacts of climate change on agriculture in sub-Saharan Africa. *Ecol Econ* 93:150–165
- Chiotti QP, Johnston T (1995) Extending the boundaries of climate change research: a discussion on agriculture. *J Rural Stud* 11:335–350
- Dubey SK, Sharma D (2018) Assessment of climate change impact on yield of major crops in the Banas River Basin, India. *Sci Total Environ* 635:10–19
- FAO (2018) *The State of Food Security and Nutrition in the World. Food and Agriculture Organization of the United Nations, Rome*
- FAO (2019) *AquaCrop | Land & Water. In: Food Agric. Organ. United Nations*
- FAOSTAT F (2018) *Statistics of the Food and Agriculture Organization of the United Nations. In: Food Agric. Organ. United Nations*
- Field CB, Barros VR (2014) *Climate change 2014–Impacts, adaptation and vulnerability: Regional aspects. Cambridge University Press*
- Gholikandi GB, Beklar BI, Amouamouha M (2021) Performance prediction and upgrading of electroanaerobic baffled reactor using neural-fuzzy method. *J Environ Chem Eng* 9:106029
- Hamed MM, Nashwan MS, Shahid S et al (2022) Inconsistency in historical simulations and future projections of temperature and rainfall: A comparison of CMIP5 and CMIP6 models over South-east Asia. *Atmos Res* 265:105927
- Hamed MM, Nashwan MS, Shahid S (2021) A novel selection method of CMIP6 GCMs for robust climate projection. *Int J Climatol*
- Heinemann AB, de HN Maia A, Dourado-Neto D, Ingram KT, Hoogenboom G (2006) Soybean (*Glycine max* (L.) Merr.) growth and development response to CO₂ enrichment under different temperature regimes. *Eur J Agron* 24(1):52–61
- Heinemann AB, Ramirez-Villegas J, Stone LF, Didonet AD (2017) Climate change determined drought stress profiles in rainfed common bean production systems in Brazil. *Agric for Meteorol* 246:64–77
- Homsy R, Shiru MS, Shahid S et al (2020) Precipitation projection using a CMIP5 GCM ensemble model: a regional investigation of Syria. *Eng Appl Comput Fluid Mech* 14:90–106
- Hosseini TSM, Hosseini SA, Ghermezcheshmeh B, Sharafati A (2020) Drought hazard depending on elevation and precipitation in Lorestan. *Iran Theor Appl Climatol* 142:1369–1377
- Kang Y, Khan S, Ma X (2009) Climate change impacts on crop yield, crop water productivity and food security—a review. *Prog Nat Sci* 19:1665–1674
- Khaleefa O, Kamel AH (2021) On the evaluation of water quality index: case study of Euphrates River, Iraq. *Knowledge-Based Eng Sci* 2:35–43
- Khan MS, Coulibaly P, Dibike Y (2006) Uncertainty analysis of statistical downscaling methods. *J Hydrol* 319:357–382
- Leemans R, Solomon AM (1993) Modeling the potential change in yield and distribution of the earth's crops under a warmed climate. *Clim Res* 79–96
- Liu YR, Li YP, Ding YK (2021) Quantifying uncertainties in temperature projections: A factorial-analysis-based multi-ensemble downscaling (FAMED) method. *Atmos Res* 247:105241
- Lobell DB, Ortiz-Monasterio JI, Asner GP et al (2005) Analysis of wheat yield and climatic trends in Mexico. *F Crop Res* 94:250–256
- Ludwig F, Asseng S (2006) Climate change impacts on wheat production in a Mediterranean environment in Western Australia. *Agric Syst* 90:159–179
- Maghrebi M, Noori R, Bhattarai R, et al (2020) Iran's Agriculture in the Anthropocene. *Earth's Futur* 8:e2020EF001547
- Naganna SR, Beyaztas BH, Bokde N, Armanuos AM (2020) On the evaluation of the gradient tree boosting model for groundwater level forecastinG. *Knowledge-Based Eng Sci* 1:48–57
- Noor M, Ismail T, Shahid S et al (2019) Development of multi-model ensemble for projection of extreme rainfall events in Peninsular Malaysia. *Hydrol Res* 50:1772–1788
- Omeje OE, Maccido HS, Badamasi YA, Abba SI (2021) Performance of hybrid neuro-fuzzy model for solar radiation simulation at Abuja, Nigeria: a correlation based input selection technique. *Knowledge-Based Eng Sci* 2:54–66
- Porter JR, Gawith M (1999) Temperatures and the growth and development of wheat: a review. *Eur J Agron* 10(1):23–36
- Qin W, Wang L, Lin A et al (2018) Comparison of deterministic and data-driven models for solar radiation estimation in China. *Renew Sustain Energy Rev* 81:579–594. <https://doi.org/10.1016/j.rser.2017.08.037>
- Reilly J, Paltsev S, Felzer B et al (2007) Global economic effects of changes in crops, pasture, and forests due to changing climate, carbon dioxide, and ozone. *Energy Policy* 35:5370–5383
- Sachindra DA, Ahmed K, Rashid MM et al (2018) Statistical downscaling of precipitation using machine learning techniques. *Atmos Res* 212:240–258
- Salman SA, Nashwan MS, Ismail T, Shahid S (2020) Selection of CMIP5 general circulation model outputs of precipitation for peninsular Malaysia. *Hydrol Res* 51:781–798
- Sharafati A, Zahabiyou B (2014) Rainfall threshold curves extraction by considering rainfall-runoff model uncertainty. *Arab J Sci Eng* 39 <https://doi.org/10.1007/s13369-014-1246-9>
- Sharafati A, Pezeshki E, Shahid S, Motta D (2020) Quantification and uncertainty of the impact of climate change on river discharge and sediment yield in the Dehbar river basin in Iran. *J Soils Sediments*
- Sharafati A, Pezeshki E (2020) A strategy to assess the uncertainty of a climate change impact on extreme hydrological events in the semi-arid Dehbar catchment in Iran. *Theor Appl Climatol* 139: <https://doi.org/10.1007/s00704-019-02979-6>
- Sharma A, Goyal MK (2020) Assessment of the changes in precipitation and temperature in Teesta River basin in Indian Himalayan Region under climate change. *Atmos Res* 231:104670
- Shiferaw B, Smale M, Braun H-J et al (2013) Crops that feed the world 10. Past successes and future challenges to the role played by wheat in global food security. *Food Secur* 5:291–317
- Shin Y, Shin Y, Hong J et al (2021) Future projections and uncertainty assessment of precipitation extremes in the Korean Peninsula from the CMIP6 Ensemble with a Statistical Framework. *Atmosphere (basel)* 12:97
- Silva V de PR da, Maciel GF, Braga CC, et al (2018) Calibration and validation of the AquaCrop model for the soybean crop grown

- under different levels of irrigation in the Motopiba region, Brazil. *Ciência Rural* 48:
- Sowers J, Vengosh A, Weinthal E (2011) Climate change, water resources, and the politics of adaptation in the Middle East and North Africa. *Clim Change* 104:599–627
- Steduto P, Raes D, Hsiao TC, et al (2009) Concepts and applications of AquaCrop: the FAO crop water productivity model. In: *Crop modeling and decision support*. Springer, pp 175–191
- Sulaiman SO, Shiri J, Shiralizadeh H et al (2018) Precipitation pattern modeling using cross-station perception: regional investigation. *Environ Earth Sci* 77:709
- Tur R, Yontem S (2021) A comparison of soft computing methods for the prediction of wave height parameters. *Knowledge-Based Eng Sci* 2:31–46
- Waha K, Krummenauer L, Adams S et al (2017) Climate change impacts in the Middle East and Northern Africa (MENA) region and their implications for vulnerable population groups. *Reg Environ Chang* 17:1623–1638
- Yang C, Fraga H, Van Ieperen W, Santos JA (2017) Assessment of irrigated maize yield response to climate change scenarios in Portugal. *Agric Water Manag* 184:178–190
- Yano T, Aydin M, Haraguchi T (2007) Impact of climate change on irrigation demand and crop growth in a Mediterranean environment of Turkey. *Sensors* 7:2297–2315

Publisher's note Springer Nature remains neutral with regard to jurisdictional claims in published maps and institutional affiliations.